This article has been accepted for publication in a future issue of this journal, but has not been fully edited. Content may change prior to final publication. Citation information: DOI 10.1109/TSG.2018.2860783, IEEE Transactions on Smart Grid

Optimal sizing of PEV fast charging stations with Markovian demand characterization

Qiang Yang, *Senior Member, IEEE,* Siyang Sun, *Student Member, IEEE,* Shuiguang Deng, *Senior Member, IEEE,* Qinglin Zhao and Mengchu Zhou, *Fellow, IEEE*

***Abstract*—Fast charging stations are critical infrastructures to enable high penetration of plug-in electric vehicles (PEVs) into future distribution networks. They need to be carefully planned to ensure meeting charging demand as well as economic benefits. Accurate estimation of PEV charging demand is the prerequisite of such planning, but a non-trivial task. This paper addresses the sizing (number of chargers and waiting spaces) problem of fast charging stations and presents an optimal planning solution based on an explicit temporal-*SoC* characterization of PEV fast charging demand. The characteristics of PEV charging demand are derived through the vehicle travel behavior analysis using available statistics. The PEV dynamics in charging stations is modelled with a Markov chain and queuing theory. As a result, the optimal number of chargers and waiting spaces in fast charging stations can be jointly determined so as to maximize the expected operator profits, considering profit of charging service, penalty of waiting and rejection, as well as maintenance cost of idle facilities. The proposed solution is validated through a case study with mathematical justifications and numerical results from simulation.**

***Index Terms*—Plug-in electric vehicle (PEV), state of charge (*SoC*), Monte Carlo simulation, Markov model, queuing theory, charging station planning.**

NOMENCLATURE

PEV related parameters

E_c	Energy consumption per kilometer of PEV battery
C_b	Maximum battery capacity
S_{nch}	PEV normal charging state
S_{fch}	PEV fast charging state
S_d	PEV driving state
S_p	PEV parking state
P_n	Typical charging power of normal charging
P_f	Typical charging power of fast charging
t_{md}	Departure time in the morning of C-PEV
t_{ma}	Arrival time in the morning of C-PEV
t_{ed}	Departure time in the evening of C-PEV
t_{ea}	Arrival time in the evening of C-PEV
t_d	Departure time of O-PEV
t_a	Arrival time of O-PEV
N_d	Valid samples that Monte-Carlo simulation generates
$SoC(t)$	SoC in the current time slot
$SoC(t+1)$	SoC in the next time slot
v	PEV average driving speed
P	Markov model of PEV
t_i	i th time slot
S_{nch}^i	Probability of normal charging in the i th time slot
S_{fch}^i	Probability of fast charging in the i th time slot
S_d^i	Probability of driving in the i th time slot
S_p^i	Probability of parking in the i th time slot
V	Expected total PEV charging demand

Charging stations related parameters

n	Total number of PEVs
λ	PEV arrival rate in the fast charging station
μ	Service rate of PEV chargers
s	Number of PEV chargers
w	Number of PEV waiting spaces
N	Maximum number of PEVs that the charging station can serve
ρ	Service capacity of the charging station
P_0	Probability that the charging station is empty
P_k	Probability that there are k PEVs in the charging station
P_N	Probability of a PEV charging request being rejected
λ_e	Arrival rate of accepted PEVs
R	Number of rejected PEV charging requests
L	Number of queued PEV charging requests

This work is supported in part by the National Key Research and Development Program of China（No. 2017YFB1400601), National Natural Science Foundation of China (51777183, 61772461), the Key Research and Development Project of Zhejiang Province (No. 2015C01027), the Natural Science Foundation of Zhejiang Province (LZ15E070001, LR18F020003) and Jiangsu Province (BK20161142).

Q. Yang and S. Sun are with the College of Electrical Engineering, Zhejiang University, Hangzhou, 310027, China (e-mail: qyang@zju.edu.cn; sunsiyang911@zju.edu.cn).

S. Deng is with the College of Computer Science and Technology, Zhejiang University, Hangzhou 310027, China (e-mail: dengsg@zju.edu.cn).

Q. Zhao is with the Faculty of Information Technology, Macau University of Science and Technology, Avenida Wei Long, Taipa, Macau, China (email: zqlict@hotmail.com).

M. Zhou is with the Department of Electrical and Computer Engineering, New Jersey Institute of Technology, Newark, NJ 07102 USA (e-mail: zhou@njit.edu).

B	Number of busy chargers
I_s	Number of idle chargers
I_w	Number of idle waiting spaces
E	Expected profit in a unit time slot of the charging station
$c_i, i \in \{1,2,3,4,5\}$	Cost factors
$s_{\max}$	Maximum allowed number of PEV chargers
$w_{\max}$	Maximum allowed number of waiting spaces
C_{sub}	Capacity of the substation that the charging station connects to
P_b	Other power load of the substation
s_V	Maximum number of PEV chargers without violating the bus voltage constraints determined by power flow calculation
δ	Confidence interval of the generated samples
r_{err}	Estimated relative error of the generated samples
$\tilde{c}$	Standard deviation of the estimated mean
$\bar{X}$	Estimated mean value of the generated samples
X_i	Generated samples
r_{err}^0	Relative error of the generated samples
N^M	Pre-defined maximum number of iterations
N^s	Number of simulation iterations
L_i	PEV state probability results after N^s iterations
ε	Convergence factor

I. Introduction

The growing concerns of fossil fuel consumption and greenhouse gas emission have prompted the rapid development of plug-in electric vehicles (PEVs) in recent years. It is anticipated that PEVs will be a fairly large segment of vehicles in USA [1] and China [2]. Currently a PEV can be charged either in a normal charging mode at its destination (e.g., home or workplace), or in a fast charging mode at fast charging stations when needed (typical charging duration of 30 minutes or less) [3]. Due to the limited driving range compared with internal combustion engine (ICE) vehicles, PEVs need to be timely charged during the trip at fast charging stations. Appropriate planning of PEV fast charging stations is of paramount importance to enable large-scale PEV deployment and the investment of charging stations will continuingly grow to meet the increasing PEV charging demand. It was reported that China aims to build 12,000 centralized charging/battery swap stations and 4.8 million scattered charging piles across the country by 2020 to service 5 million PEVs [2].

The investigation of PEV fast charging station planning has received much research attention in recent years. The existing work has mainly addressed such a planning problem from two aspects: sitting (i.e., location), and sizing (i.e., capacity) of charging stations. The former (e.g., [4-10]) determines the optimal placement of fast charging stations aiming to ensure the economic and security operation of electrical distribution networks whilst meeting the transportation network constraints. The studies [11-14] have addressed the optimal sizing problem of PEV fast charging stations from the total power capacity perspective. In particular, the authors in [11] exploit the optimal planning of PEV fast charging stations in a highway transportation network based on a capacitated-flow refueling location model and a mixed-integer linear programming model. An integrated planning framework is presented in [12] to minimize the overall PEV charging infrastructure cost in urban areas by using the Voronoi diagram and particle swarm optimization. In [13], a stochastic planning model is developed for PEV charging stations equipped with single output multiple cables charging spots to minimize the equivalent annual cost considering the coordinated charging strategy. The authors in [14] present a mixed integer non-linear optimization approach for optimal placement and sizing of fast charging stations, considering the station construction cost, PEV energy loss, power grid loss as well as the locations of electric substations and urban roads.

However, the optimal configuration of fast charging stations (i.e., the number of chargers and waiting spaces) and service performance assessment (e.g., queued and rejected PEV charging requests) have not been explicitly investigated in the literature. The solutions in [3, 15-17] adopt queuing theory to determine the optimal number of charging facilities in order to meet the PEV charging demand as well as promote the service quality of charging stations. However, it should be noted that these solutions simply assume that the PEV charging demand is known as a priori, or follows a simple pattern of PEV charging requests (e.g., a fixed PEV arrival rate). This may make the solutions problematic in practice as the arrival pattern of PEV charging requests can vary due to dynamic travel behaviors and state of charge (*SoC*) conditions. In addition, the maintenance cost of idle charging facilities also needs to be fully considered during the cost-benefit analysis of fast charging stations.

Therefore, the accurate modeling and estimation of PEV fast charging demand are needed to determine the optimal capacity and configuration of fast charging stations. However, the stochastic and diverse PEV travel patterns make the explicit mathematical formulation of PEV charging demand a non-trivial task [18], which has been exploited in recent years [19-24]. However, the aforementioned solutions have mainly focused on the normal charging mode (i.e., charged at home or workplace), and hence cannot be directly adopted in fast charging station planning. Also, these solutions only consider simplified PEV travel behaviors (e.g., the starting time of travel and the daily driving distance) without the explicit formulation of temporal travel patterns and *SoC* dynamics.

To this end, this paper addresses the challenges of optimal sizing of PEV fast charging stations based on the explicit characterization of PEV fast charging demand by using Markov modeling techniques. The number of chargers and waiting spaces in fast charging stations are jointly optimized to

This article has been accepted for publication in a future issue of this journal, but has not been fully edited. Content may change prior to final publication. Citation information: DOI 10.1109/TSG.2018.2860783, IEEE Transactions on Smart Grid

maximize the expected station profit, considering the service profit, queuing and rejection cost, as well as maintenance cost of idle facilities. The main technical contributions are summarized as follows: (1) a temporal-*SoC* analysis of PEV travel behaviors is adopted based on Monte-Carlo simulation and Markov model techniques to obtain the estimation of PEV fast charging demand; and (2) the PEV charging dynamics is formulated using the M/M/s/N queuing model and the station configuration (i.e., the number of chargers and waiting spaces) is jointly optimized through a comprehensive benefit-cost analysis considering the service quality and operational constraints of power distribution networks. The proposed approach is implemented and extensively assessed through the numerical analysis of a case study.

The rest of the paper is organized as follows: Section II presents the temporal-*SoC* analysis of PEV charging demand; Section III formulates the optimal sizing problem of fast charging stations using a queuing model; the proposed solution is further implemented through a case study in Section IV; finally, the conclusive remarks are given in Section V.

II. Temporal-SoC Analysis of PEV Charging Demand

This section presents the temporal-*SoC* analysis of PEV travel behaviors and fast charging demand through the determination of PEV travel behaviors and state transitions. The overall process of Markovian demand characterization is illustrated in Fig. 1 and discussed in the following subsections.

A. Preliminaries

It is reported that in the UK, 61% of vehicles are privately owned primarily for commuting between home and the working place, which have two trips in the morning and evening, respectively (i.e., C-PEV); others are owned by companies and used primarily for business purposes or owned by those retired from work or who are unemployed, which have multiple trips over a day (i.e., O-PEV). For the sake of simplicity, only the first departure and the last arrival of O-PEVs are considered in this work [25]. The typical energy consumption per kilometer E_c of PEV battery is 0.159 *kWh/km* and the maximum battery capacity C_b (*kWh*) follows the normal distribution $N(\mu,\sigma^2)$ ($\mu=28.5$ and $\sigma=14.7$) with the maximum and minimum value of *max*=72.0 and *min*=10.0, respectively [26], as given in (1).

$$f(x)=\frac{1}{\sqrt{2\pi}\sigma}e^{-\frac{(x-\mu)^2}{2\sigma^2}} \tag{1}$$

At any given time slot, PEVs can operate at one of the following four states: normal charging state (S_{nch}), fast charging state (S_{fch}), driving state (S_d) and parking state (S_p). It is assumed that the operational PEV state remains unchanged within a time slot (30 minutes per time slot, i.e., there are in total 48 time slots in a day). The typical charging power, P_n of 3.3kW (220V/15A) and P_f of 50kW (400V/125A) are adopted with constant charging rate for normal and fast charging modes, respectively [16]. PEVs are immediately charged in a normal mode upon the arrivals at home. In this work, it is considered that *SoC* exceeding 0.8 (over charging) and less than 0.2 (over discharging) should be avoided during the PEV travel and charging process in order to protect the battery lifetime [27].

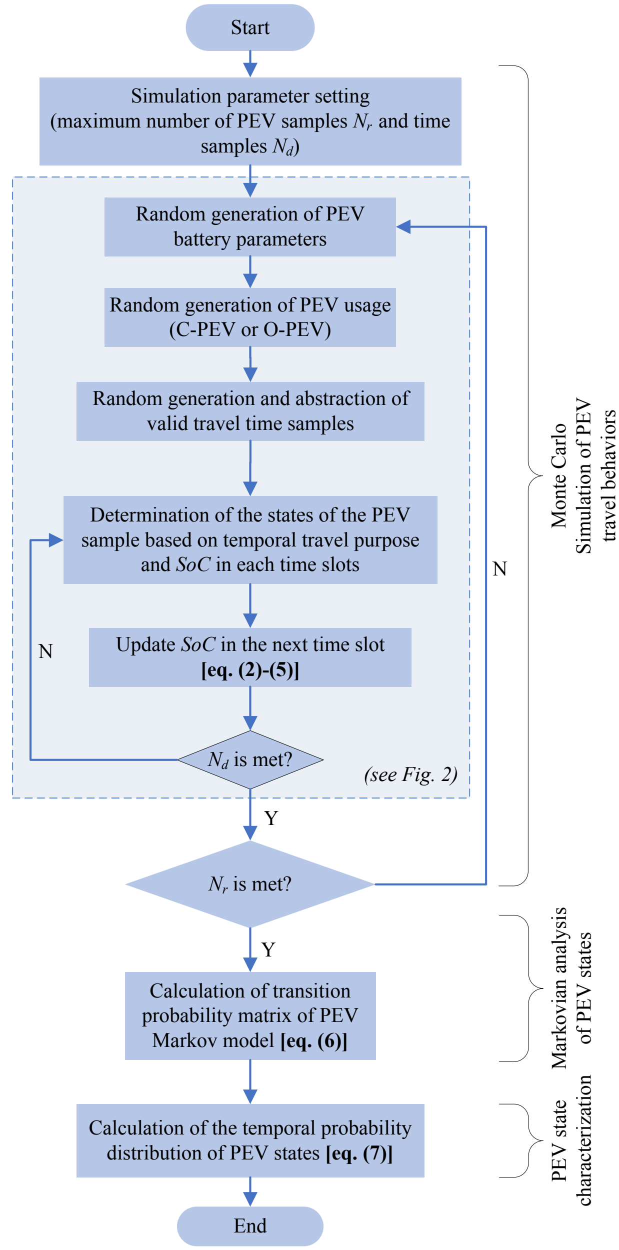

Fig.1: The temporal-*SoC* analysis of PEV charging demand

PEV travel patterns are considered as same as those of ICE vehicles. Thus, various available travel data statistics [29-31], e.g., National Household Travel Survey (NHTS), can be adopted to characterize PEV temporal travel patterns. By the use of data normalization, maximum likelihood estimation, as well as curve-fitting techniques, the departure and arrival time in the morning and evening of C-PEV (t_{md} , t_{ma} , t_{ed} and t_{ea}), and the departure and arrival time of O-PEV (t_d and t_a) follow the normal distribution (1), as shown in Table I.

This article has been accepted for publication in a future issue of this journal, but has not been fully edited. Content may change prior to final publication. Citation information: DOI 10.1109/TSG.2018.2860783, IEEE Transactions on Smart Grid

Table I: PEV temporal travel patterns

	t_{md}	t_{ma}	t_{ed}	t_{ea}	t_d	t_a
Mean μ ($h : min$)	6:52	8:00	16:52	17:29	13:51	17:29
Standard deviation σ (h)	1.3	3.4	2.3	3.25	5.2	3.25

B. Monte Carlo simulation of PEV behaviors

The Monte Carlo simulation technique is used to generate the purpose of usage and the battery capacity of individual PEV samples based on the probability distribution and the constraints aforementioned. The Monte Carlo process does not terminate until N_d valid random travel time samples are generated, in the case that the generated capacity C_b does not meet the maximum (*max*) and minimum (*min*) constraints.

Consequently, the proposed temporal-*SoC* analysis firstly considers the current simulation time slot to preliminarily determine the temporal travel purpose of individual PEV samples (i.e. ***Scenario 1-6*** for C-PEV and ***Scenario 1-4*** for O-PEV), then the PEV travel behavior is further examined based on the current *SoC* according to the assumptions of this work (i.e. ***Case 1*** or ***2***), as shown in Table II and Fig. 2. Moreover, different temporal scenarios over a day for C-PEV and OPEV are shown in Fig. 3.

Once the travel behavior of individual PEV samples in a time slot is determined by the algorithm, the initial *SoC* of the next time slot $SoC(t+1)$ can be updated according to the current PEV state and generated PEV parameters using (2) - (5). This process is repeated for all time slots over a day.

$$SoC(t+1) = SoC(t) - \frac{vE_c}{2C_b} \tag{2}$$

$$SoC(t+1) = SoC(t) + \frac{P_f}{2C_b} \tag{3}$$

$$SoC(t+1) = SoC(t) + \frac{P_n}{2C_b} \tag{4}$$

$$SoC(t+1) = SoC(t) \tag{5}$$

Here, once the simulation time reaches 24:00 (i.e., the end of a day), then it is updated to be 0:00 of a new day with the same *SoC*, implying that the proposed modeling approach can continuously simulate the PEV travel behaviors for all N_d days, and *SoC* only need to be initialized once for individual PEV samples before the simulation (the initial *SoC* is set to 0.5). Such steps are carried out for each PEV sample in each time slot until the termination condition is met. More details of the adopted temporal-*SoC* analysis of PEV travel behaviors can be found in in our previous work [32].

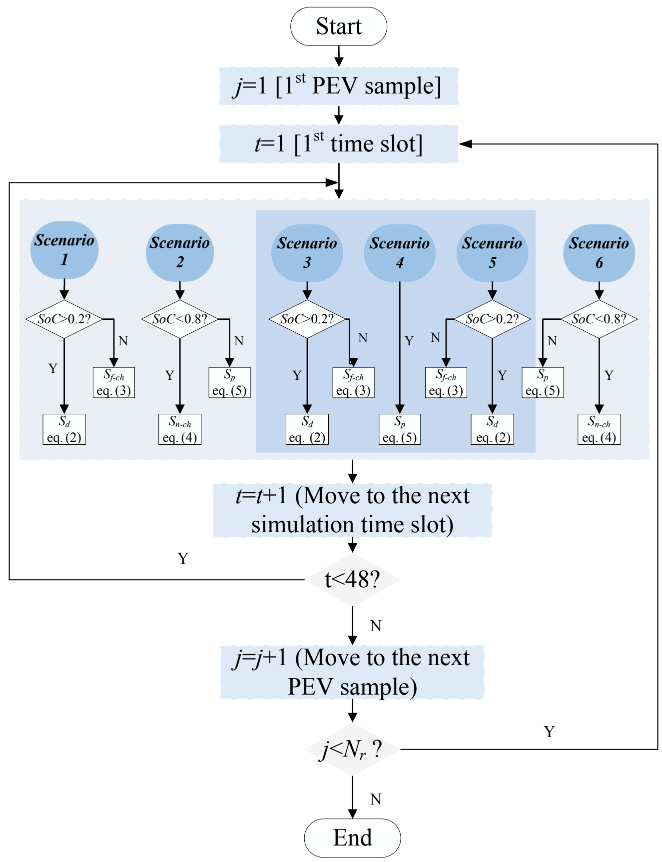

Fig. 2: The flowchart of PEV state modeling

Table II: Temporal PEV travelling scenarios

	Scenario	1		2		3	4	5	6
C-PEV	Time	$t < t_{ea}(j-1) - 24$		$t_{ea}(j-1) - 24 < t < t_{md}(j)$		$t_{md}(j) < t < t_{ma}(j)$	$t_{ma}(j) < t < t_{ed}(j)$	$t_{ed}(j) < t < t_{ea}(j)$	$t_{ea}(j) < t < t_{md}(j+1) + 24$
	Travel purpose	Driving to home or fast charging		Parking or normal charging at home		Driving to the workplace or fast charging	Parking at the workplace	Driving to home or fast charging	Parking or normal charging at home
	Case	1	2	1	2	As same as *Scenario 1*	As same as *Scenario 2, Case 2*	As same as *Scenario 1*	As same as *Scenario 2*
	SoC	> 0.2	≤ 0.2	< 0.8	≥ 0.8				
	State	S_d	S_{fch}	S_{nch}	S_p		S_p		

	Scenario	1	2	3	4
O-PEV	Time	$t < t_a(j-1) - 24$	$t_a(j-1) - 24 < t < t_d(j)$	$t_a(j) < t < t_d(j)$	$t_a(j) < t < t_d(j+1) + 24$
	Case	As same as *Scenario 1* of C-PEV	As same as *Scenario 2* of C-PEV	As same as *Scenario 1* of C-PEV	As same as *Scenario 2* of C-PEV
	SoC				
	State				

This article has been accepted for publication in a future issue of this journal, but has not been fully edited. Content may change prior to final publication. Citation information: DOI 10.1109/TSG.2018.2860783, IEEE Transactions on Smart Grid

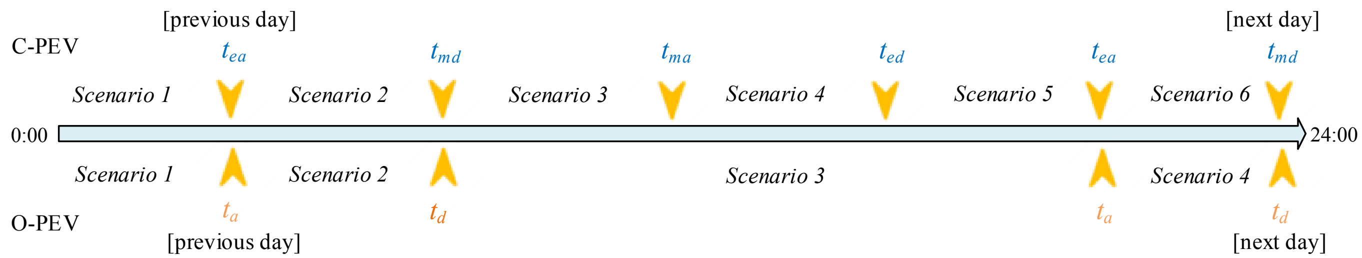

Fig. 3: The illustration of different temporal scenarios for C-PEVs and O-PEVs

C. Markov model of PEVs

Based on the Markov model theory, the Markov transition probability matrix for all possible state transitions is given as:

$$P=\begin{bmatrix} p_{11} & p_{12} & p_{13} & p_{14} \\ p_{21} & p_{22} & p_{23} & p_{24} \\ p_{31} & p_{32} & p_{33} & p_{34} \\ p_{41} & p_{42} & p_{43} & p_{44} \end{bmatrix} \tag{6}$$

where p_{ij} denotes the transition probability from state i to state j. Total 48 time slots (assuming 30 minutes per slot) per day imply that each element of this Markov transition probability matrix is a 1×48 vector.

The Markov transition probability matrix P can be obtained based on the approach presented in Fig. 1. Through the travel pattern modeling of all PEV samples, the PEV state in each time slot for individual PEV samples can be explicitly derived. According to the definition of the Markov transition probability matrix, the total number of each PEV state appearances in each time slot in the simulation is added up, in which the appearance count of its next PEV state for each PEV state is also calculated. Thus, for every PEV state in every time slot, the Markov transition probability matrix of PEVs over a day can be derived statistically, as shown in Fig. 4.

It is noted that some transitions may not occur between certain PEV states, which are excluded during the calculation of Markov matrix P. Thus, the transition probabilities among different PEV states in any given time slot can be explicitly determined.

D. Probability distribution of PEV states

Given the PEV state distribution at t_0 as (S^0_{nch} S^0_{fch} S^0_d S^0_p), the PEV state distribution in the next time slot (S^1_{nch} S^1_{fch} S^1_d S^1_p) can be derived based on the Markov model via (7):

$$(S^1_{nch},S^1_{fch},S^1_d,S^1_p)=(S^0_{nch},S^0_{fch},S^0_d,S^0_p)\times P \tag{7}$$

Through iterating the aforementioned process for all time slots ($t_0 \sim t_{48}$), the PEV states for all time slots over a day can be derived. Given the initial (i.e., t_0=0:00) state distribution of (0.3309, 0.0084, 0.0391, 0.6218), Fig. 5 presents the average probabilities of PEV states over a day obtained from the aforementioned Monte-Carlo simulation.

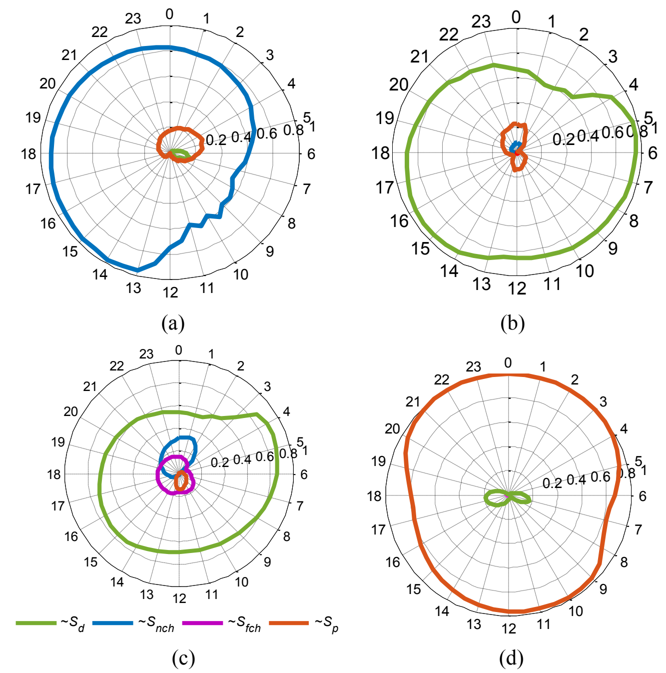

Fig. 4: The Markov transition probability matrix of PEVs (a): from normal charging state; (b): from fast charging state; (c): form driving state; (d): from parking state

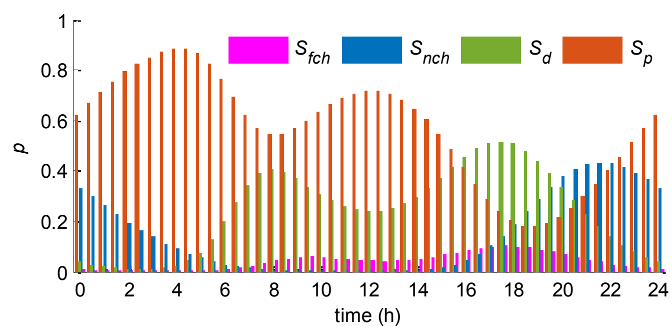

Fig. 5: The probability of different PEV states over a day

Through the PEV probabilities in each time slot, if we know the total number of PEVs n in a certain geographical area, the expected PEV charging demand V at time slot t_i can be obtained according to (8), where the first and last terms represent the expected normal charging and fast charging demand, respectively.

$$V=P_n\times n\times S^{t_i}_{nch}+P_f\times n\times S^{t_i}_{fch} \tag{8}$$

It should be noted that through the proposed Markov model of temporal PEV states, once the initial state distribution is

This article has been accepted for publication in a future issue of this journal, but has not been fully edited. Content may change prior to final publication. Citation information: DOI 10.1109/TSG.2018.2860783, IEEE Transactions on Smart Grid

given, the PEV states in all time slots over a day can be derived based on (8). Such analytical approach is generic and scalable, and hence can be adopted in different cases, e.g., different PEV populations and operational patterns.

III. Optimal Sizing of Fast Charging Stations

In this work, queuing theory is adopted to characterize the stochastic charging patterns of PEVs based on their arrivals at fast charging stations. Once the locations of the fast charging stations in the transportation system are given, the vehicle traffic flow can be determined, and hence the arrival pattern of PEV charging requests can be calculated.

Here, the PEV arrivals follow a Poisson process with an arrival rate λ, and the PEV charging duration follows an exponential distribution with an average duration $1/\mu$ (i.e., 30 minutes). Based on the derived expected PEV fast charging demand (Section II), the arrival rate in individual time slots can be obtained. Let s be the number of PEV chargers, w be the number of waiting spaces, and $N=s+w$ be the maximum number of PEVs that a charging station can serve, an M/M/s/N model [14] is adopted to model the PEV fast charging stations. Its Markov chain is illustrated in Fig. 6 (b).

In such M/M/s/N model, all PEV chargers work independently, and in the case that all chargers are busy upon a PEV arrival, the PEV is queued at one of the waiting spaces and served in a first-come-first-served (FCFS) manner once a charger is available; if all the waiting spaces are occupied, the charging request is rejected and the rejected PEV leaves.

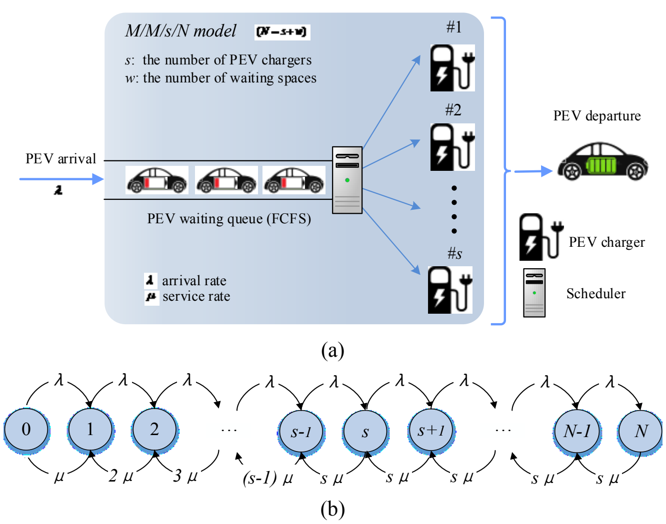

Fig. 6: The illustration of (a) The M/M/s/N model and (b) Markov chain of PEV fast charging station

Based on the Markov chain shown in Fig 6 (b), the balance state of this system can be expressed by a set of differential equations as given in (9):

$$\begin{cases} \mu P_1 = \lambda P_0 \\ (k+1)\mu P_{k+1} + \lambda P_{k-1} = (\lambda + k\mu)P_k, (1 \le k \le s) \\ s\mu P_{k+1} + \lambda P_{k-1} = (\lambda + s\mu)P_k, (s < k < N) \\ \lambda P_{k-1} = s\mu P_N \end{cases} \tag{9}$$

where P_0 represents the probability that the charging station is empty, P_k denotes the probability that there are k PEVs in the charging station, and $\sum_{k=0}^{N} P_k = 1$.

The service capacity of the charging station is defined as (10):

$$\rho = \frac{\lambda}{s\mu} \tag{10}$$

Therefore, the equilibrium state of P_0 and P_k can be derived using (11) and (12) based on the recurrence relations in (9):

$$P_0 = \begin{cases} \left[\sum_{k=0}^{s-1} \frac{1}{k!}(s\rho)^k + \frac{s^s}{s!}\left(\frac{\rho(\rho^s - \rho^N)}{1-\rho}\right) \right]^{-1}, \rho \ne 1 \\ \sum_{k=0}^{s-1} \frac{1}{k!} s^k + \frac{s^s}{s!}(w+1), \rho = 1 \end{cases} \tag{11}$$

$$P_k = \begin{cases} \frac{1}{k!}(s\rho)^k P_0, k \le s \\ \frac{s^s}{s!}\rho^k P_0, k > s \end{cases} \tag{12}$$

The probability of a PEV charging request being rejected is given as P_N, and hence the rate of accepted PEVs to be charged can be expressed as

$$\lambda_e = \lambda(1 - P_N) \tag{13}$$

The number of rejected PEV charging requests, R, queued requests, L, and busy chargers B, are expressed as:

$$R = \lambda P_N \tag{14}$$

$$L = \sum_{k=s+1}^{N} (k-s)P_k \tag{15}$$

$$B = s\rho(1 - P_N) \tag{16}$$

The maintenance cost of idle facilities is also considered in this work, and the number of idle chargers and waiting spaces can be expressed as follows, respectively:

$$I_s = s - B \tag{17}$$

$$I_w = w - L \tag{18}$$

Finally, the expected profit of the PEV fast charging station in a unit time slot E can be expressed as:

$$E = c_1 B - (c_2 L + c_3 R + c_4 I_s + c_5 I_w) \tag{19}$$

where $c_i, i \in \{1,2,3,4,5\}$ denote the cost factors.

Based on the aforementioned formulation, the optimal planning of charging station capacity aims to maximize the profit through determining the appropriate number of chargers s and waiting spaces w, subject to the constraints as follows:

$$\max \sum_{t=1}^{48} E(t) \qquad s.t. \begin{cases} 1 \le s \le s_{\max} \\ 0 \le w \le w_{\max} \end{cases} \tag{20}$$

where $s_{\max}$ is the maximum allowed number of PEV chargers due to electric power system constraints, and $w_{\max}$ is the maximum allowed number of waiting spaces due to the space

This article has been accepted for publication in a future issue of this journal, but has not been fully edited. Content may change prior to final publication. Citation information: DOI 10.1109/TSG.2018.2860783, IEEE Transactions on Smart Grid

limitation of a charging station.

The maximum allowed number of PEV chargers $s_{\max}$ can be obtained by (21):

$$s_{\max} \le \min\left\{\frac{C_{sub}-P_b}{P_f}, s_V\right\} \tag{21}$$

where $\frac{C_{sub}-P_b}{P_f}$ indicates the maximum number of chargers without exceeding the total allowed capacity regulated by the substation transformer; and s_V represents the maximum number of chargers without violating the constraint of bus voltage deviation (e.g., 5%).

IV. CASE STUDY

This section carries out a set of case studies to implement and justify the effectiveness of the proposed solution. The IEEE 53-bus test distribution feeder is adopted in this case study and the network parameters (e.g., transformer capacity and voltage fluctuation) are available in [37]. The available transportation statistics of Beijing, China are adopted for PEV charging demand characterization, as given in Table III [33]. Consequently, the PEV charging demand can be estimated based on the temporal-*SoC* analysis.

Table III: Transportation statistics of Beijing used in the experiment

PEV type	M1	N1
Market share *ms*	ms^{M1} =87.2%	ms^{N1} =12.8%
Proportion of PEV usage	C-PEV	O-PEV
	r_C =82.7%	r_O =17.3%
Travel times	Mean	Standard deviation
t_{md} of C-PEVs	μ_{md} =7:34	σ_{md} =2.37
t_{ma} of C-PEVs	μ_{ma} =8:20	σ_{ma} =1.86
t_{ed} of C-PEVs	μ_{ed} =17:14	σ_{ed} =1.80
t_{ea} of C-PEVs	μ_{ea} =18:03	σ_{ea} =2.34

A. Convergence analysis

In this work, N_d valid samples are generated to represent the diverse PEV travel patterns. Based on the termination criteria of Monte Carlo simulation [34], if the confidence interval δ is twice of the standard deviation of the estimated mean, i.e., $\delta = 2\tilde{\varsigma}$, the estimated relative error r_{err} of the generated samples with the confidence level of 95.45% is expressed as:

$$r_{err} = \frac{2\tilde{\varsigma}}{\bar{X}} \tag{22}$$

where $\tilde{\varsigma}$ and $\bar{X}$ are the estimations for the standard deviation and the mean value of the generated samples, as shown in (23) and (24):

$$\tilde{\varsigma} \quad \frac{\;}{N-1}\left[\frac{1}{N}\sum_{i=1}^{N} X_i^2 - \bar{X}^2\right] \tag{23}$$

$$\bar{X} = \eta = \frac{1}{N}\sum_{i=1}^{N} X_i \tag{24}$$

The Monte Carlo simulation terminates once the pre-defined relative error r_{err}^0 is met, indicating that the generated travel time samples are converged within the error range of $\pm r_{err}^0$ with the confidence level of 95.45%.

Here, N_d is set to be 20 000, and the relative errors of the generated travel time samples from Monte Carlo simulation for t_{md} , t_{ma} , t_{ed} , t_{ea} and t_d are 0.0051, 0.0061, 0.0033, 0.0034 and 0.0093, respectively. It is observed that all generated travel time samples can be converged within $\pm r_{err}^0$ =0.01 with 95.45% confidence interval. This indicates that these generated samples can be considered independent, and hence can statistically represent the PEV travel pattern characteristics.

The calculation of characterizing PEV travel behaviors terminates under either of the two following conditions:

(i) The pre-defined maximum number of iterations N^M is met;

(ii) The mismatch of the PEV state probability results between any two sequential iterations is sufficiently small, as given in (25) [18]:

$$\max\left|\frac{\sum_{i=1}^{N^s} L_i}{N^s} - \frac{\sum_{i=1}^{N^s-1} L_i}{N^s-1}\right| < \varepsilon \tag{25}$$

where N^s represents the number of simulation iterations, L_i is used to record the PEV state probabilities after N^s iterations, and ε is the convergence factor. Here, ε is set to be 0.0001 and N^M is initially set to be 10000.

Condition (ii) ensures that all of the results obtained from the Monte Carlo simulation can be converged within $\pm\varepsilon$. Fig. 7 provides the average probabilities of four PEV states after N^s iterations in 48 time slots over a day (each curve corresponds to a time slot). It is shown in the simulation that condition (ii) is met when N^s reaches about 1,800. This indicates that N^M can be set to 2,000, such that the simulation convergence is guaranteed with significantly reduced computational complexity. To clearly demonstrate the convergence performance of the algorithm with the given parameters, the result of PEV state probabilities for the time slot t_{37} (i.e., 19:00-19:30) is provided as an example inside the subfigures with the maximum iterations N^M =10,000.

Finally, the computational complexity of the proposed temporal-*SoC* analysis is assessed. It takes 445.276 seconds (about 7.5 minutes) using MATLAB (ver. R2014a) on a laptop computer with a 2.50GHz Intel(R) Core(TM) i7-6500U CPU and a 4.00 GB RAM.

This article has been accepted for publication in a future issue of this journal, but has not been fully edited. Content may change prior to final publication. Citation information: DOI 10.1109/TSG.2018.2860783, IEEE Transactions on Smart Grid

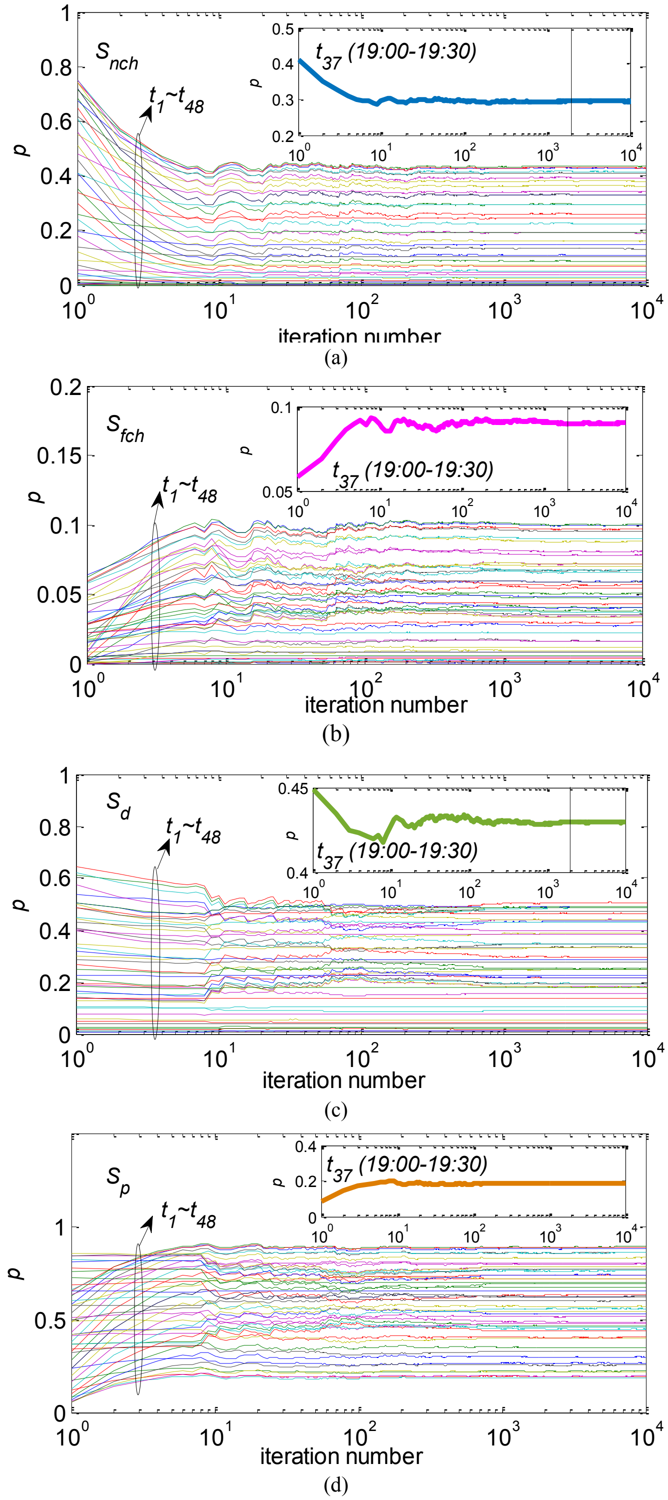

Fig. 7: Average PEV state probabilities with different number of iterations (a): normal charging state; (b): fast charging state; (c): driving state; (d): parking state

B. Optimal sizing of a fast charging station

Now the performance of the proposed solution is assessed through numerical analysis for two different scenarios: peak and time-varying PEV arrival rate. The simulation parameters of $c_1 = 5(\$)$, $c_2 = 1(\$)$, $c_3 = 2(\$)$, $c_4 = 0.5(\$)$, $c_5 = 0.05(\$)$, and $s_{\max} = 20, w_{\max} = 20$ are adopted as suggested in [20]. The PEV traffic flow is assumed to be $n = 100$ per time slot and the PEV charging performance (i.e. probabilities of rejected charging requests, waiting PEVs and charged PEVs) as well as the charging station profit are evaluated.

1) Peak arrival rate scenario:

The sizing of a charging station is firstly examined for the scenario with highest arrival intensity of PEV charging requests, i.e. peak arrival rate. It can be obtained from previous results (in Fig. 4) that the largest probability of PEV charging requests is 0.1028, and hence the maximum arrival rate under the peak charging time is $\lambda = 10.28$ per slot for the evaluated scenario with 100 PEVs in the traffic flow. Fig. 8 (a) presents the result of charging station profit against a different number of chargers and waiting spaces in the peak arrival rate scenario. Through solving (20), the optimal number of PEV chargers and waiting spaces of 14 and 10 respectively can be identified with the maximum profit of \$48.36. Fig. 8 (b) presents the assessment result of charging performance in terms of the probability for a PEV to be rejected, charged and queued upon an arrival at a charging station with 14 chargers and 10 waiting spaces. It can be observed that nearly none of the arrival PEV charging requests are rejected since the capacity is planned based on the peak arrival rate. However, such capacity planning strategy can result in underutilization of charging facilities due to idle chargers and waiting spaces. This is confirmed by the result in Fig. 8 (c) showing the charging station profit over a day with the total profit of \$716.86. The deficit of charging station is observed within the period of 11:00 pm to 7:00 am due to the maintenance cost of idle facilities.

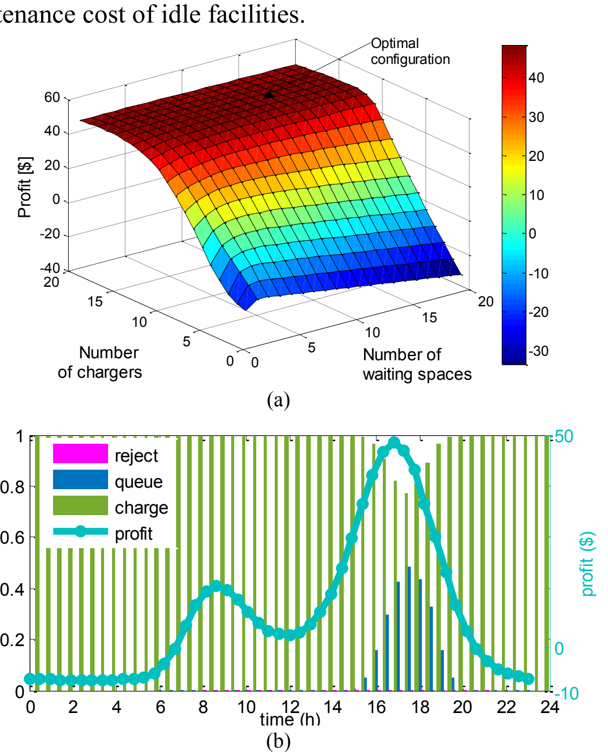

Fig. 8: Performance assessment in the peak arrival rate scenario (a) charging station profit in the peak arrival rate time slot vs. the number of chargers and waiting spaces; (b) the probabilities of rejected, charged, queued PEV upon arrival and station profit over a day (*s*=14, *w*=10)

This article has been accepted for publication in a future issue of this journal, but has not been fully edited. Content may change prior to final publication. Citation information: DOI 10.1109/TSG.2018.2860783, IEEE Transactions on Smart Grid

2) Time-varying arrival rates scenario:

Here, the optimal charging station sizing considering time-varying rate of PEV charging requests is studied. As the arrival rate for individual time slots can be obtained from the charging demand model, the profit for any time slot (in total 48 time slots) can be calculated, and hence the optimal number of chargers and waiting spaces with the maximum profit over a day can be identified as 11 chargers and 7 waiting spaces with the total profit of \$859.43. Fig. 9 (a) provides the numerical result of accumulated profit of the charging station against the number of chargers and waiting spaces over a day. The charging performance under such planned capacity (i.e. s=11 and w=7) as well as the profit over a day are presented in Fig. 9 (b) and (c), respectively. Compared with the peak arrival rate scenario, such planning solution can effectively make the appropriate trade-off between the charging performance and the charging station profit.

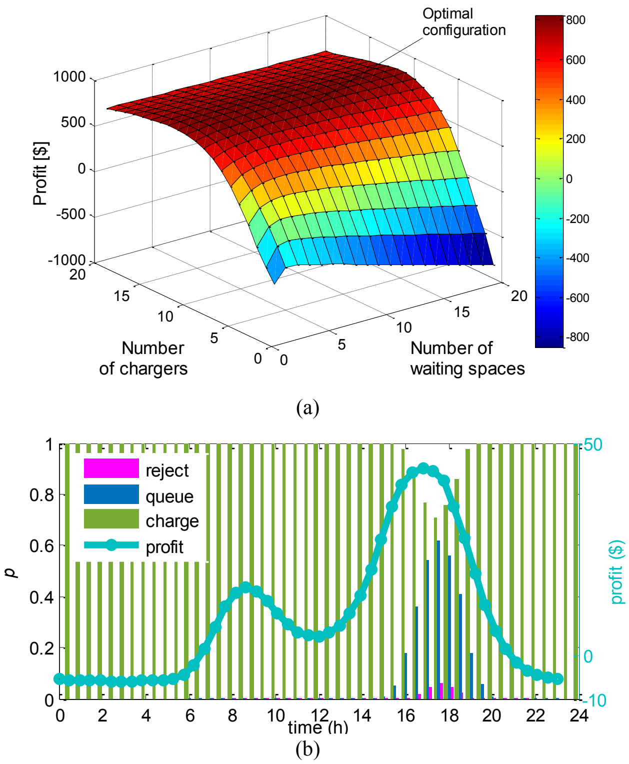

Fig. 9: Performance assessment in the time-varying arrival rates scenario (a) accumulated profit for different chargers and waiting spaces over a day; (b) the probability of rejected, charged, queued PEV upon arrival and the station profit over a day (s=11, w=7)

Finally, Fig. 10 presents the charging service performance assessment and charging station profit against different arrival rates of PEV charging requests. It is observed that the charging performance degrades along with the increase of arrival rate and the profit decreases when the arrival rate exceeds the charging station service capacity due to the significant rejected charging requests. This further highlights the importance of accurate characterization and estimation of PEV charging demand for appropriate sizing of fast charging stations.

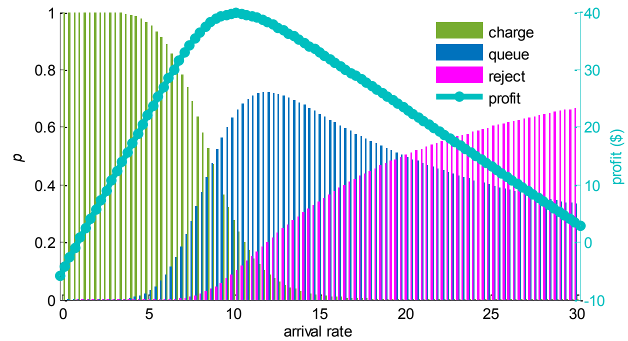

Fig. 10: The probabilities of service performance and the station profit vs. different PEV arrival rates

V. Conclusions and Future Work

This paper presents a novel approach to optimally plan the sizing (number of chargers and waiting spaces) of PEV fast charging stations based on the explicit formulation of PEV fast charging demand. The demand is firstly derived through the temporal-*SoC* analysis based on the available statistics. The arrival pattern of charging requests to the charging station can be formulated based on a Markov chain and queuing theory. The optimal number of chargers and waiting spaces in the fast charging stations are jointly optimized by considering the cost-benefit performance from both operator and PEV user perspectives. The proposed solution is evaluated through a set of case studies for peak rate and time-varying arrival rate scenarios through simulations. The numerical results confirm the effectiveness of the proposed solution.

In the future, the proposed solution can be further improved through incorporating realistic distribution network case studies using a massive number of field statistics, e.g., PEV travel patterns and battery parameters. This work can be also extended to the exploitation of temporal-spatial planning approach to simultaneously optimize the capacity and placement of charging stations considering the presence of distributed generators [35-36] and coupling constraints of power distribution and transportation networks. Finally, further research effort is needed to investigate the scheduling strategies of PEV charging behaviors considering the vehicle to grid (V2G) interactions as well as the dynamic pricing schemes.

References

[1] J. C. Mukherjee and A. Gupta, "Distributed charge scheduling of plug-in electric vehicles using inter-aggregator collaboration," *IEEE Trans. Smart Grid*, vol. 8, no. 1, pp. 331-341, Jan. 2017.

[2] Global Information, Inc., "China EV charging station and charging pile market report, 2017-2020," March 21, 2017.

[3] M. Ismail, I. S. Bayram, M. Abdallah, E. Serpedin, and K. Qaraqe, "Optimal planning of fast PEV charging facilities", *IEEE Smart Grid and Renewable Energy (SGRE)*, March 2015.

[4] A. Y. S. Lam, Y. W. Leung and X. Chu, "Electric vehicle charging station placement: formulation, complexity, and solutions," *IEEE Trans. Smart Grid*, vol. 5, no. 6, pp. 2846-2856, Nov. 2014.

[5] X. Wang, C. Yuen, N. U. Hassan, N. An, and W. Wu, "Electric vehicle charging station placement for urban public bus systems," *IEEE Trans. Intell. Transp. Sys.*, vol. 18, no. 1, pp. 128-139, Jan. 2017.

[6] C. Luo, Y. F. Huang and V. Gupta, "Placement of EV charging stations—balancing benefits among multiple entities," *IEEE Trans. Smart Grid*, vol. 8, no. 2, pp. 759-768, March 2017.

[7] J. Cavadas, G. Homem de Almeida Correia, and J. Gouveia, “A MIP model for locating slow-charging stations for electric vehicles in urban areas accounting for driver tours”, *Transportation Research Part E: Logistics and Transportation Review*, vol. 75, pp. 188-201, 2015.

[8] N. Shahraki, H. Cai, M. Turkay, and M. Xu, “Optimal locations of electric public charging stations using real world vehicle travel patterns”, *Transportation Research Part D Transport & Environment*, vol. 41, pp. 165–176, 2015.

[9] R. Riemann, D. Z. Wang, and F. Busch, “Optimal location of wireless charging facilities for electric vehicles: Flow-capturing location model with stochastic user equilibrium”, *Transportation Research Part C Emerging Technologies*, vol. 58, pp. 1–12, 2015.

[10] S. H. Chung and C. Kwon, “Multi-period planning for electric car charging station locations: A case of Korean Expressways”, *European Journal of Operational Research*, vol. 242, no. 2, pp. 677–687, 2015.

[11] H. Zhang; S. Moura; Z. Hu; Y. Song, "PEV fast-charging station siting and sizing on coupled transportation and power networks," *IEEE Trans. Smart Grid* , vol. PP, no.99, pp.1-1, 2017.

[12] H. Zhang, Z Hu, Z. Xu, Y. Song, “An integrated planning framework for different types of PEV charging facilities in urban area”, *IEEE Trans. Smart Grid*, vol. 7, no. 5, pp. 2273 – 2284, Sept. 2016.

[13] H. Zhang; Z. Hu; Z. Xu; Y. Song, "Optimal planning of PEV charging station with single output multiple cables charging spots," *IEEE Trans. Smart Grid*, vol.PP, no.99, pp.1-10, 2017.

[14] P. Sadeghi-Barzani, A. Rajabi-Ghahnavieh, and H. Kazemi-Karegar, “Optimal fast charging station placing and sizing,” *Applied Energy*, vol. 125, pp. 289–299, 2014.

[15] C. Kong, I. S. Bayram, M. Devetsikiotis, “Revenue optimization frameworks for multi-class PEV charging stations”, *IEEE Access*, Vol. 3, Nov. 2015.

[16] G. Li, X. P. Zhang, “Modeling of plug-in hybrid electric vehicle charging demand in probabilistic power flow calculations”, *IEEE Trans. Smart Grid*, vol. 3, no. 1, pp. 492-499, March 2012.

[17] L. Feng, S. Ge, H. Liu, L. Wang, and Y. Feng, “The planning of charging stations on the urban trunk road,” *IEEE ISGT’12*, pp. 1-4, May 2012.

[18] W. Yao, C. Y. Chung, F. Wen, M. Qin, and Y. Xue, “Scenario-based comprehensive expansion planning for distribution systems considering integration of plug-in electric vehicles,” *IEEE Trans. Power Systems*, vol. 31, no. 1, pp. 317-328, Jan. 2016.

[19] Y. Mu, J. Wu, N. Jenkinsa, H. Jia, C. Wang, “A spatial–temporal model for grid impact analysis of plug-in electric vehicles”, *Applied Energy*, vol. 114, pp. 456–465, Feb. 2014.

[20] K. Qian, C. Zhou, M. Allan, Y. Yuan, “Modeling of load demand due to EV battery charging in distribution systems”, *IEEE Trans. Power Systems*, Vol. 26, no. 2, pp. 802-810, May 2011

[21] B. Zhou, F. Yao, T. Littler, H. Zhang, "An electric vehicle dispatch module for demand-side energy participation", *Applied Energy*, vol. 177, pp. 464-474, 2016.

[22] H. Xu, F. Ouyang, H. Liu, et al, “A probability load modeling method for the charging demand of large-scale PEVs accounting users’ charging willingness”, *Int. J Elec. Power,* vol. 82, pp. 331-338, 2016.

[23] Harris, Chioke B., and M. E. Webber. "An empirically-validated methodology to simulate electricity demand for electric vehicle charging." *Applied Energy*, vol. 12, pp. 172-181, 2014.

[24] A. Weis, P. Jaramillo, and J. Michalek, "Estimating the potential of controlled plug-in hybrid electric vehicle charging to reduce operational and capacity expansion costs for electric power systems with high wind penetration." *Applied Energy*, vol. 115, no.4, pp. 190-204, 2014.

[25] National Statistics, Department for Transport. Transport Statistics Bulletin Vehicle Licensing Statistics: 2010, April 9, 2011, [Online]. Available: http://www2.dft.gov.uk/pgr/statistics/datatablespublications/vehicles/licensing/latest/vls2010.pdf.

[26] Transport Research & Innovation Portal, “Mobile energy resources in grids of electricity”, [Online]. Available: http://www.transport-research.info/sites/default/files/project/documents/20140203_154622_76425_Deliverable_2.1_Modelling_Electric_Storage_devices_for_Electric_Vehicles.pdf

[27] F. Marra, G. Yang, C. Træholt, J. Østergaard and E. Larsen, "A decentralized storage strategy for residential feeders with photovoltaics," *IEEE Trans. Smart Grid*, vol. 5, no. 2, pp. 974-981, March 2014.

[28] A. M. A. Haidar, K. M. Muttaqi, “Behavioral characterization of electric vehicle charging loads in a distribution power grid through modeling of battery chargers”, *IEEE Trans. Industry Applications*, vol. 52, no. 1, pp. 483-492, Jan./Feb. 2016.

[29] U.S. Department of Transportation Federal Highway Administration, “Summary of travel trends: 2009 National Household Travel Survey”, [Online]. Available: http://nhts.ornl.gov/2009/pub/stt.pdf.

[30] T. Wu, Q. Yang, Z. Bao, and W. Yan, “Coordinated energy dispatching in microgrid with wind power generation and plug-in electric vehicles”, *IEEE Trans. Smart Grid*, vol. 4, no. 3, pp. 1453-1463, Sept. 2013.

[31] Beijing Transportation Research Center, “Annual Report on Beijing's Transportation Development in 2011”, [Online]. Available: http://www.bjtrc.org.cn/InfoCenter/NewsAttach/aeb7c878-d31e-4f08-982f-3c17c717c87b.pdf.

[32] S. Sun, Q. Yang, W. Yan, "A novel Markov-based temporal-SoC analysis for characterizing PEV charging demand," *IEEE Trans. Industrial Informatics*, vol. 14, no.1, pp.156-166, Jan. 2018.

[33] Beijing Transportation Research Center, [Online]. Available: http://www.bjtrc.org.cn/InfoCenter/NewsAttach/aeb7c878-d31e-4f08-982f-3c17c717c87b.pdf.

[34] C. Jungemann, S. Yamaguchi, H. Goto, “Convergence estimation for stationary ensemble Monte Carlo simulations”, *IEEE Journal of Technology Computer Aided Design TCAD*, Feb. 2013.

[35] W. S. Im, C. Wang, W. Liu, *et al*, “Distributed virtual inertia based control of multiple photovoltaic systems in autonomous microgrid,” *IEEE/CAA Journal of Automatica Sinica*, vol. 4, no. 3, pp. 512-519, 2017

[36] B. Huang, Y. Li, H. Zhang, Q. Sun, “Distributed optimal co-multi-microgrids energy management for energy internet,” *IEEE/CAA Journal of Automatica Sinica*, vol. 3, no. 4, pp. 357-364, 2016.

Qiang Yang (M’03-SM’18) received Ph.D. degree in Electronic Engineering and Computer Science from Queen Mary, University of London, London, U.K., in 2007 and worked in the Department of Electrical and Electronic Engineering at Imperial College London, U.K., from 2007 to 2010. He visited University of British Columbia and University of Victoria Canada as a visiting scholar in 2015 and 2016. He is currently an Associate Professor at College of Electrical Engineering, Zhejiang University, China, and has published more than 120 technical papers, applied 40 national patents, co-authored 2 books and several book chapters. His research interests over the years include communication networks, smart energy systems, and large-scale complex network modeling, control and optimization. He is the member of IEEE, IET and the Senior Member of China Computer Federation (CCF).

Siyang Sun (S’18) received the B.S. degree in automation from Zhejiang University, Hangzhou, China, in 2014, where he is currently pursuing the Ph.D. degree in electrical engineering. His current research interests include electric vehicles grid integration, charging station planning and demand response.

This article has been accepted for publication in a future issue of this journal, but has not been fully edited. Content may change prior to final publication. Citation information: DOI 10.1109/TSG.2018.2860783, IEEE Transactions on Smart Grid

Shuiguang Deng is a full professor at the College of Computer Science and Technology in Zhejiang University. He received the BS and PhD both in Computer Science from Zhejiang University in 2002 and 2007, respectively. He worked at Massachusetts Institute of Technology (MIT) in 2014 and at Stanford University in 2015 as a visiting scholar. His research interests include Service Computing, Mobile Computing, and Business Process Management. Up to now he has published more than 80 papers in journals such as IEEE TOC, TPDS, TSC, TCYB and TNNLS, and refereed conferences. He is the Associate Editor of the journal IEEE Access and IET Cyber-Physical Systems: Theory & Applications. He is a senior member of IEEE.

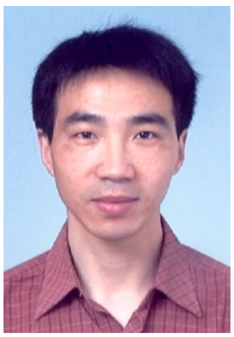

Qinglin Zhao received the PhD degree from the Institute of Computing Technology, Chinese Academy of Sciences, Beijing, China, in 2005. From May 2005 to August 2009, he did research in The Chinese University of Hong Kong and The Hong Kong University of Science and Technology, Hong Kong. Since September 2009, he has been with the Faculty of Information Technology, Macau University of Science and Technology, Macau, China. His research interests include wireless communications and networking, software-defined wireless networks, IoT and Blockchain.

Mengchu Zhou (M'90–SM'93–F'03) received the B.S. degree in control engineering from the Nanjing University of Science and Technology, Nanjing, China, in 1983, the M.S. degree in automatic control from the Beijing Institute of Technology, Beijing, China, in 1986, and the Ph.D. degree in computer and systems engineering from Rensselaer Polytechnic Institute, Troy, NY, USA, in 1990. He joined the New Jersey Institute of Technology, Newark, NJ, USA, in 1990, where he is currently a Distinguished Professor of Electrical and Computer Engineering. He has over 620 publications including 12 books, 320+ journal papers (240+ in the IEEE TRANSACTIONS), and 28 book-chapters. His current research interests include Petri nets, Internet of things, big data, Web services, and manufacturing, transportation, and energy systems. Dr. Zhou was a recipient of the Humboldt Research Award for the U.S. Senior Scientists, the Franklin V. Taylor Memorial Award, and the Norbert Wiener Award from the IEEE Systems, Man and Cybernetics Society. He is the Founding Editor of the IEEE Press Book Series on Systems Science and Engineering. He is a Fellow of the International Federation of Automatic Control and the American Association for the Advancement of Science.